Arch. Mech., 44, 1, pp. 43–54, Warszawa 1992

Differential law for anisotropic hardening evolution

M. BOUCHER (CACHAN) and J. P. CORDEBOIS (PARIS)

THE AIM of this paper is to define a model which describes the evolution of the yield surface during the plasticity. We propose a model which is completely different from the classical approach, as far as its concept is concerned. It consists in describing the yield surface evolution in terms of the velocity. The yield function is not directly known but is obtained by integrating a differential law starting from an initial surface. A very simple evolution law is used; the complexity of the induced anisotropy is obtained by incremental accumulation.

1. Introduction

PRESENTLY, in order to realize more realistic numerical simulations of forming processes, a lot of works turn on the anisotropic aspect of the plastic behaviour of metallic materials.

The computations which use laws based on the Von Mises or Hill criteria with isotropic or kinematical hardening do not allow, in most cases, to get quite satisfactory results. In fact, induced anisotropy is not fully taken into account. If the study is restricted to standard materials, the constitutive law is given by means of the yield surface. The accuracy of the description of this surface determines the quality of the constitutive law. In a general way, a criterion of plasticity expressed by

$$\mathcal{F}(\sigma, \ldots) = 0,$$

where $\mathcal{F}$ is a numerical function of a tensorial variable σ and hardening parameter leads to a particular kind of strain hardening directly connected with the shape of $\mathcal{F}$. The strain hardening can evolve only within a determined family thanks to the evolution of the parameters. The analytic functions $\mathcal{F}$ usually employed are too simple to interpret the complexity of the phenomenon. If more complex functions are used, it is possible to have a slight amelioration of the description but not satisfactory because the limitation of this kind of model is always present.

Our point of view consists in approaching the function $\mathcal{F}$ no longer with an explicit expression but by means of an integration, along the loading path, of a differential law starting from an initial function. Then, it is possible to obtain, by incremental accumulation, the description of strong induced anisotropy, even if the evolution law is simple.

2. Experimental results

The tests used to perfect the model were developed in several laboratories. The exploitation of the set of results needs a classification of these tests by means of a description of the loading path. This is done in a way which allows to have a physical interpretation.

2.1. Characteristics of the loading path

An intrinsic characterization of symmetric second order tensors is proposed with the help of the following expression

$$[\mathbf{T}] = \mathcal{J}_T[\mathbf{Q}][\mathbf{T}'][\mathbf{Q}]^t,$$

where $[\mathbf{T}]$ is the matrix which represents the tensor $\mathbf{T}$ on a basis; $\mathcal{J}_T = \sqrt{\mathrm{tr}(\mathbf{T} \circ \mathbf{T})}$ is the intensity of $\mathbf{T}$; $[\mathbf{Q}]$ is the matrix which gives the orientation of $\mathbf{T}$ with respect to the material: it is the matrix of the rotation which allows to go from the initial basis to the principal basis of $\mathbf{T}$; $[\mathbf{T}']$ represents the type of $\mathbf{T}$ (uniaxial tensor, isotropic tensor ...): it is a diagonal matrix whose components are the principal stresses divided by $\mathcal{J}_T$.

In the first step, the model is used for pressing of thin metal sheets and then, it is convenient to use a plane stress condition. In this case, a single scalar parameter α, $\alpha \in [0, \pi[$ is necessary to give the position of $\mathbf{T}$. α is the angle between the principal direction associated with the eigenvalue of greatest magnitude and the material direction which has been previously chosen. The two eigenvalues T_1' and T_2' of $\mathbf{T}'$ satisfy:

$$T_1'^2 + T_2'^2 = 1.$$

So, there is an angle Ψ which represents the type of $\mathbf{T}'$:

$$T_1' = \cos\Psi, \quad T_2' = \sin\Psi, \quad \Psi \in [-\pi/4, \pi/4] \cup]3\pi/4, 5\pi/4].$$

2.2. Experimental tests

Tensile tests

These tests, for which $\Psi = 0$, are developed for various values of α contained between 0 and $\pi/2$. Figure 1 shows the results for a sheet steel E275D, [5]. The curves obtained for different values of α are approximately identical.

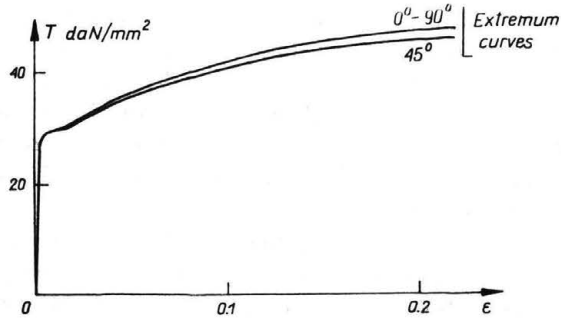

FIG. 1. Tensile tests on sheet steel E275D.

The confirmation of this observation is obtained for two other types of sheet steel. So, in the first step, we shall suppose that the plastic behaviour is independent of α and Ψ.

Unidimensional tests [5]

Each test is characterized by a specific value of Ψ. For example:

tensile test: $\Psi = 0$,

uniform biaxial expansion: $\Psi = \pi/4$,

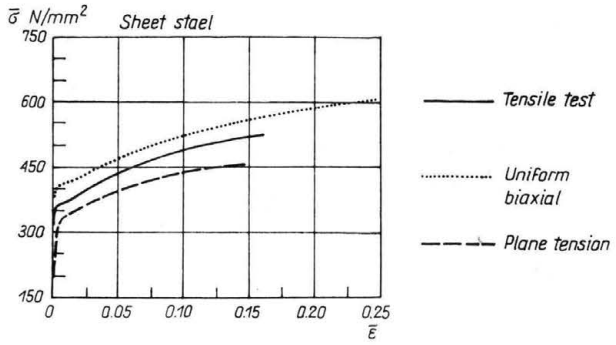

FIG. 2. Unidimensional tests.

plane tension: $\Psi = \text{arctg}(1/2)$.

Figure 2 shows that the hardening modulus for a given value of the equivalent plastic strain varies not much. So, always in the first step, we shall suppose that the plastic behaviour is independent of Ψ.

Tension-torsion tests [2, 3]

The previous tests give the evolution of a particular point of the yield surface. They do not allow to define the evolution of the whole surface in the full stress space which needs multiaxial tests. Such tests are not yet developed in the most general case. The first approach consists in the tension-torsion tests which allow to get the evolution of the section of the yield surface by the plane $(\sigma_{11}, \sigma_{12})$.

The set of the tests and the principal results are related in detail in [4]. Here, the most important conclusions are recalled:

The evolution of the yield surface presents the following properties:

• A distortion which appears at the very beginning of the predeformation. It is obtained with a pointed end in the neighbourhood of the loading point and a flat end at the opposite side (Fig. 3). Especially, this last aspects shows that the Bauschinger effect is very important.

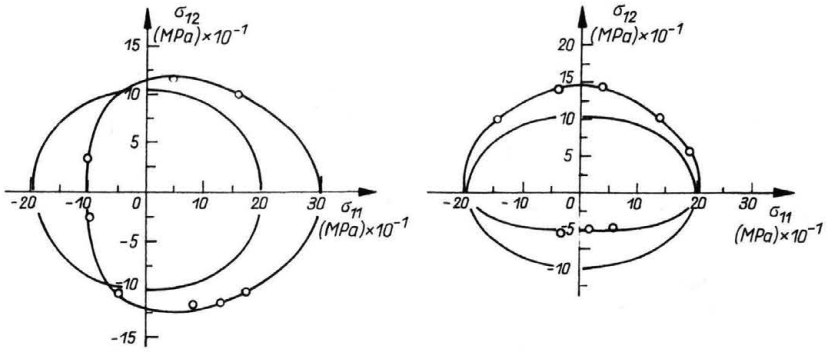

FIG. 3. Predeformation in tension or torsion.

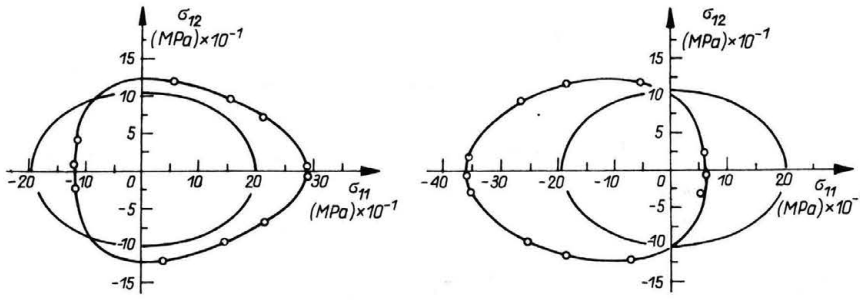

FIG. 4. Predeformation in torsion foll ıy a compressive test.

• A cross-effect which consists in "swelling" perpendicularly to the loading direction (Fig. 3). More precisely, we call cross-effect the strain hardening which happens along the Direction 2 when the loading acts parallely to the Direction 1. These directions are taken in a strain meaning: if the plastic strain rates are $\dot{\varepsilon}_p^{(1)}$ and $\dot{\varepsilon}_p^{(2)}$, we have

$$\mathrm{tr}(\dot{\varepsilon}_p^{(1)} \circ \dot{\varepsilon}_p^{(2)}) = 0.$$

In particular, the combination of the two former effects leads to a global swelling of the domain which is the representation of isotropic hardening.

These effects are much more obvious when the predeformation is done according to the symmetry axes of the yield surface. For mixed predeformations, these effects are always present but, in addition, the yield surface tends to become symmetrical with respect to the loading direction.

For intermittent loadings, there is a very fast return of the surface to the neighbourhood of the former point of loading. Figure 4 shows the results for a linear loading path formed by a tensile loading followed by an elastic unloading and a compressive loading. The return of the pointed end obtained at the end of the tensile loading when the compressive loading is beginning is perceptible at the very time when a new pointed end is developing in the neighbourhood of the compression point.

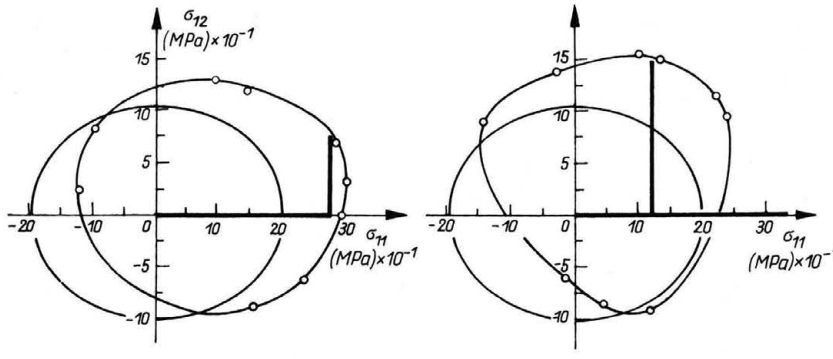

FIG. 5. Predeformation in tension followed by a torsion test.

Figure 5 shows the other case of this phenomenon for a nonlinear loading path. This kind of loadings is typical in deep drawing performed in several steps.

For intermittent loadings with two types of loads separated by an elastic unloading, it is interesting to compare the behaviour during the second step and the one which would be obtained with a direct loading of the second type, that is to say, without predeformation of the first type. Of course, the comparison is done for equivalent plastic strains and the behaviour is different, but if the loadings go on, these results tend to a common limit, [6] and [7].

3. Modelling

3.1. Hypothesis

Only a state of plane stress is considered.

The presentation is supported by tension-torsion tests but the model can directly be generalized to a general plane stress state.

The influence of the parameter α is neglected. So, we suppose that the result observed for tensile tests is true for all types of loading.

In this presentation, we also neglect the influence of Ψ on the behaviour.

These hypothesis allows to build a model with only one parameter $\mathcal{J}_T$.

3.2. Fundamental remark

The proposed model takes place in the theory of standard materials combined with a criterion of plasticity. Consequently, the normal to the yield surface at the point of loading, is collinear with the plastic strain rate. To compute, it is necessary to choose a base in the space of the symmetrical second order tensors which preserves the canonical scalar product. In other words, it is necessary to preserve the property of orthogonality. An orthonormal base being chosen in the physical space, the application which associates a symmetrical second order tensor σ with the element $(\sigma_{11}, \sigma_{22}, \sigma_{33}, \sqrt{2}\sigma_{12}, \sqrt{2}\sigma_{13}, \sqrt{2}\sigma_{23})$ of R^6, meets our requirement.

In any other point of the surface, the normal is characteristic of the direction of the plastic strain rate which would happen if the concerned point became a loading point. For this reason, for each point, we define the evolution of the yield surface along the corresponding normal.

3.3. Strain hardening parameters

The observations made during the previous tests lead to introducing three kinds of strain hardening:

Direct strain hardening σ_d, whose rate $\dot{\sigma}_d$ gives the yield surface evolution along its normal $\mathbf{N}^*$ at the loading point:

$$\dot{\sigma}_d = \dot{\mathbf{M}}^* \cdot \mathbf{N}^*.$$

Crossed strain hardening σ_l whose rate $\dot{\sigma}_l$ gives the evolution of the yield surface in the direction $\mathbf{N}_l$, perpendicular to $\mathbf{N}^*$

$$\dot{\sigma}_l = \dot{\mathbf{M}}_l \cdot \mathbf{N}_l.$$

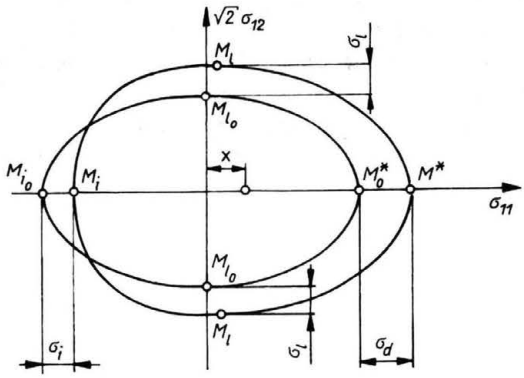

FIG. 6. Strain hardening σ_d, σ_i, σ_l.

Indirect strain hardening σ_i whose rate $\dot{\sigma}_i$ gives the evolution of the yield surface in the direction $\mathbf{N}_i$, opposite to $\mathbf{N}^*$ (Fig. 6).

$$\dot{\sigma}_i = \dot{\mathbf{M}}_i \cdot \mathbf{N}_i.$$

These different strain hardenings can be expressed by functions of the equivalent plastic strain $\bar{\varepsilon}$ in the following manner:

$$\sigma_d = g_d(\bar{\varepsilon}), \quad \sigma_i = g_i(\bar{\varepsilon}), \quad \sigma_l = q_l(\bar{\varepsilon}).$$

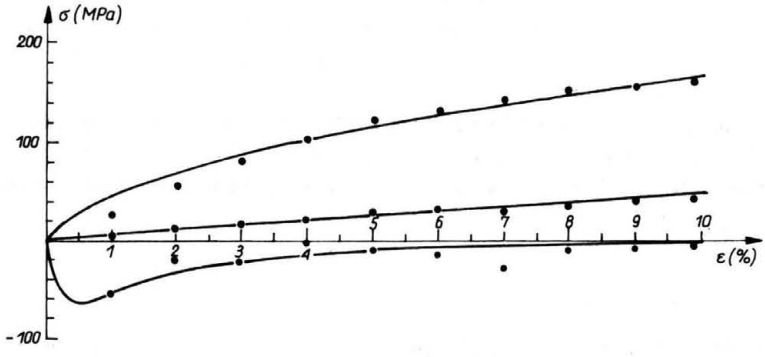

FIG. 7. Identification of strain hardening.

In conformity with the previous hypothesis, the functions g_d, g_i and g_l are independent of α and Ψ. So, they are known from the tensile test. It is clear that the former strain hardenings give the evolution of the surface for the points M^*, M_i and M_l. The three hardening functions g_d, g_i and g_l have been identified with tension-torsion tests on thin tubes in AU4G by tensile predeformation, Fig. 7.

3.4. Monotonous loading

For any point of the surface, the evolution along the normal **N** is given by a strain hardening which is a combination of two among these three particular strain hardenings. If the point M is between M^* and one of the points M_l, then it is a combination of direct strain hardening and crossed (called also latent) strain hardening.

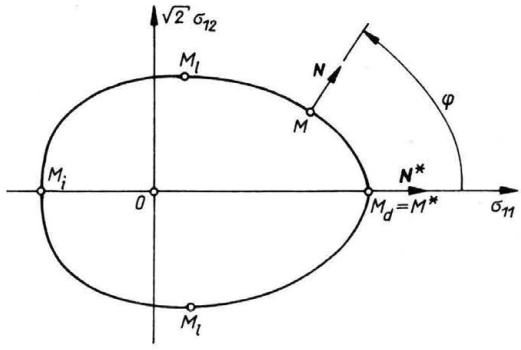

FIG. 8. Description of the yield surface.

The coefficients of this combination depend on the angle φ between the normal at M and the normal at the loading point M^*. Of course, if M is between M_i and one of the points M_l, a combination of indirect strain hardening and latent strain hardening is used, Fig. 8.

This procedure can be justified by means of the system of slip planes which is at the basis of the theory of plasticity. We think that the system of slip planes which would be active if M was a loading point, may be divided into two parts. The first part is a subset of the system of slip planes which are active with a loading at M^* and the sliding is direct or indirect, according to the position of M between M^* and M_l, or M_i and M_l. In the model, this subset is a function of the scalar product of $\mathbf{N}^*$ and $\mathbf{N}$, that is to say

$$\cos\varphi = \mathbf{N}^* \cdot \mathbf{N}.$$

In the same way, the second part proceeds from the system of slip planes at the points M_l. In order to have a symmetrical evolution rate, we use a function of $|\sin\varphi|$.

The strain hardening rate at the point M has a component on the normal **N** which can be expressed in the form:

$$\dot{\sigma}(M,t) = \dot{\sigma}(\varphi,\bar{\varepsilon}) = \dot{\sigma}_d(\bar{\varepsilon})f_d(\varphi) + \dot{\sigma}_i(\bar{\varepsilon})f_i(\varphi) + \dot{\sigma}_l(\bar{\varepsilon})f_l(\varphi),$$

f_d, f_i and f_l are functions of φ through $\cos\varphi$ and $|\sin\varphi|$. They must satisfy simple conditions like

$$f_d(\varphi) = 0 \text{ when } \cos\varphi \le 0, \quad f_d(0) = 1, \quad f_d(\varphi) = f_d(-\varphi),$$
$$f_i(\varphi) = 0 \text{ when } \cos\varphi \ge 0, \quad f_i(\pi) = 1, \quad f_i(\varphi) = f_i(-\varphi),$$
$$f_l(\varphi) \ge 0 \ \forall\varphi, \quad f_l(0) = f_l(\pi) = 0, \quad f_l(\pi/2) = 1, \quad f_l(\varphi) = f_l(\pi - \varphi)$$

and they are obtained by identification of the experimental results.

The tests used for the identification of the three hardening functions allow to propose the following expressions for the influence function f_d, f_i and f_l:

$$f_d(\varphi) = (\langle \cos\varphi \rangle^+)^2, \quad f_i(\varphi) = (\langle \cos\varphi \rangle^-)^2, \quad f_l(\varphi) = \sin^2\varphi.$$

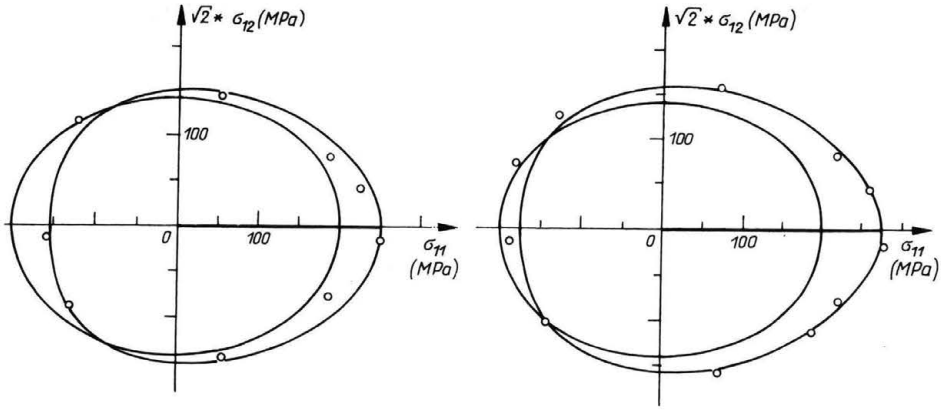

FIG. 9. Simulation of predeformation in tension.

We have $f_d(\varphi) + f_i(\varphi) + f_l(\varphi) = 1$, $\forall\varphi$. This means that the strain hardening rate at the point M is a convex combination of the three former particular strain hardening rates. That leads to the theoretical yield surfaces of Fig. 9.

It is worth noting that only the scalar product of the normal **N** and the normal **N*** is used, and this keeps a meaning for general plane stress conditions and is not specific for the tension-torsion state.

3.5. Comeback effect

First of all, it is useful to determine the terminology. We talk about plastic loading path when the stress history leads to a plastic strain rate which is not equal to zero for any time. So, a general loading path may be the succession of plastic loading paths and elastic loading paths. In this case, we shall employ the name of intermittent loading path.

Orthogonal intermittent loading path

In the evolution of the yield surface, the comeback effect is very significant for intermittent loading path. So, after a predeformation up to the point A, there is an elastic loading followed by a new plastic loading path starting from the point C, Fig. 10. Here, we consider the case where the normals in A and in C are orthogonal. We may say that there is a discontinuity of $\pi/2$ for the plastic loading path.

Figure 10 shows, in continuous line, the yield surface obtained at the end of the predeformation, and also at the beginning of the second plastic loading path. This surface represents the microscopic plastic state of the set of the slip planes at the considered material point for a plastic loading path ending in A. This microscopic state is in agreement with the loading point A. When the loading path goes from A to C, there is no evolution of the plasticity, the microscopic state of the slip planes does not change, so it is not in

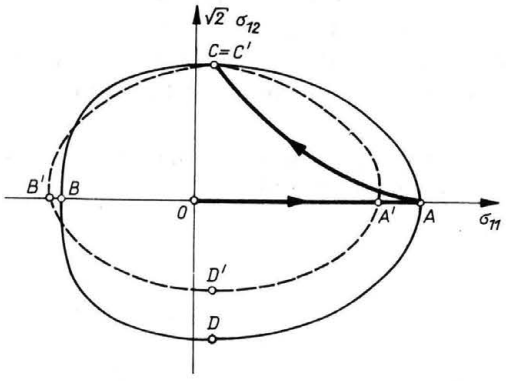

FIG. 10. Comeback effect.

agreement with the loading point C. Therefore, the yield surfaces (continuous line) is not in agreement with the loading point C. The yield surface which would be obtained with a linear plastic loading path ending at the point C and which would be in agreement with the loading point C is shown by the dashed line.

For a new plastic loading path starting from C, both the yield surface tend to a common limit. In other words, the points A, B, C and A', B', C' tend to common points. For example, let us consider the evolution of the point C. When the loading point is A, there is a latent hardening in C which depends on the equivalent plastic strain $\bar{\varepsilon}_A$. It is equivalent to a direct hardening obtained for a linear plastic loading path ending at the point C with an equivalent plastic strain defined by

$$\sigma_d(\bar{\varepsilon}_C) = \sigma_l(\bar{\varepsilon}_A).$$

So, there are two parts in the evolution of the point C. The first one, which occurs when the loading point is in A, is governed by the latent hardening curve. The second one, which corresponds to the new plastic loading path with C as loading point, is governed by a hardening curve obtained by a translation $(\bar{\varepsilon}_A - \bar{\varepsilon}_C)$ of the direct hardening curve, Fig. 11. The translation corresponds to the fact that the single parameter of history is the plastic equivalent strain $\bar{\varepsilon}_A$.

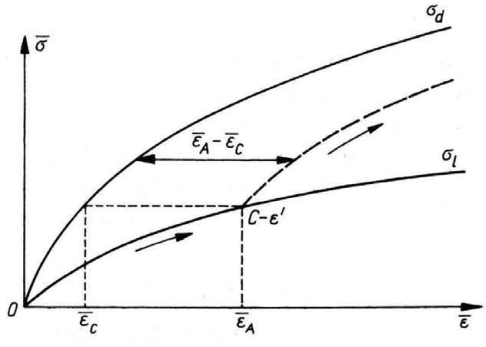

FIG. 11. Evolution of the point C.

About the evolution of the point A, we remark that the system of the slip planes given by $\mathbf{N}_A$ leads to a strain hardening much greater than the one represented by A', which could exist for a linear plastic loading path ending at C. Moreover, the strain hardenings are different because it is direct hardening in the first case and a latent one in the second case.

When we consider the new plastic loading starting from C, there are two parts of the evolution of the point A. We have supposed that A and A' tend to a common point.

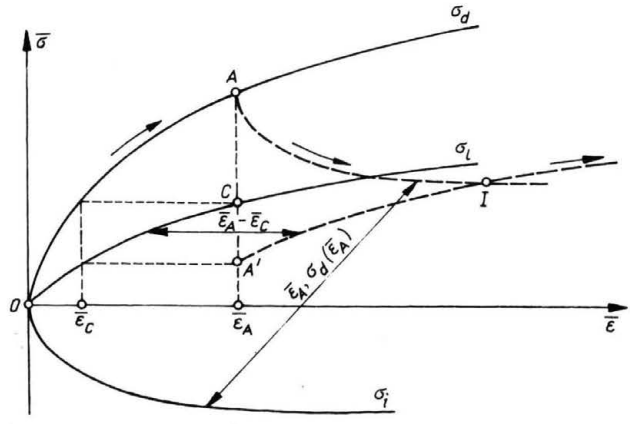

FIG. 12. Evolution of the point A.

The first part of the evolution happens before A and A' reach this common point: it is the comeback effect. During this effect, there is an indirect strain hardening in A. About the point A', it is always the same latent strain hardening which continues. At the meeting of both the points, the comeback effect for A disappears, there is only a latent strain hardening which goes on, Fig. 12.

Similar reasoning may be applied to the evolution of the points B and D, [4].

General intermittent loading path

In this case, after a predeformation up to the point M_1^*, there is an elastic loading path followed by a new plastic loading path starting from M_2^* with the normals in M_1^* and M_2^* which are no longer orthogonal, Fig. 13. The discontinuity of the plastic loading path is given by the angle φ^*. The evolution of the yield surface, when we consider a new plastic loading path starting from C, is obtained in the same way as in the previous case with the use of the points A, B and C for which the normals to the yield surface satisfy the conditions

$$\mathbf{N}_A \perp \mathbf{N}_2^*, \quad \mathbf{N}_B = -\mathbf{N}_A, \quad \mathbf{N}_D = -\mathbf{N}_2^*.$$

The only difference with the previous case is that these three points A, B and D are not obtained directly during the first part of the loading but are the result of an integration.

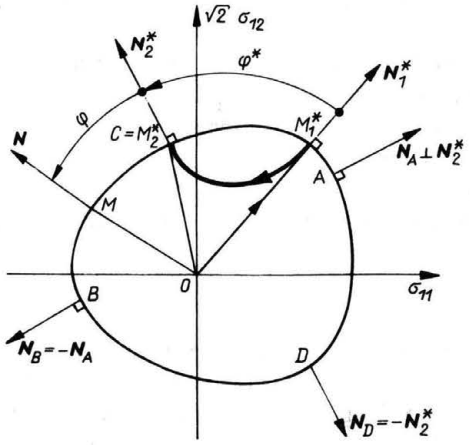

FIG. 13. General comeback effect.

4. Simulations

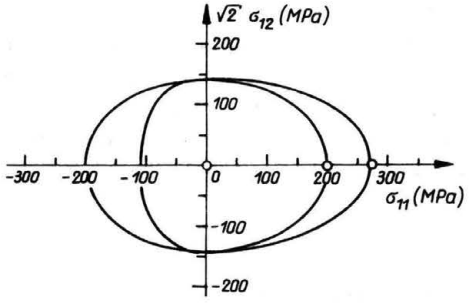

FIG. 14. Simulation of a predeformation of tension.

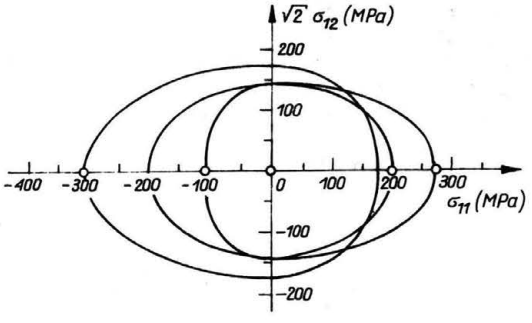

FIG. 15. Simulation of the comeback effect.

Figure 14 gives the simulation of the evolution of the yield surface for a predeformation of tension.

Figure 15 shows the simulation of the comeback effect in the case of a predeformation of tension followed by a compressive loading path.

As we can see, for both the simulation presented we obtain a good description of the distorsion of the yield surface, the latent hardening and the comeback effect. Moreover, this numerical results are in a good agreement with the experimental results. Of course, it will be necessary to make other simulations in order to verify the model presented.

5. Conclusions

The model is based on a description of three types of hardening: direct, indirect and latent hardening. The hypothesis, which have been used, lead to an identification of the model which requires the knowledge of three curves, one for each type of hardening, and it is sufficient to describe the physical behaviour of the material.

The model is built on a macroscopic interpretation of microscopic phenomena connected with the set of the slip planes. The comeback effect has been also justified.

The incremental character of the model allows to apply it to any loading path.

It is possible to get an extension of the model to three-dimensional loading path without additional difficulty. Nevertheless, it is necessary to obtain some more information on the latent hardening in the whole subspace of directions perpendicular to the direction of the plastic strain rate at the loading point. To this end, a series of tests must be done, in particular those of combined tension and torsion with internal or external pressure.

The introduction of the model in computer codes for numerical simulations of the forming processes must improve the results in comparison with those obtained by means of the models based on the von Mises or Hill criteria.

References

1. A. BENCHOUIKH, A. DOGUI and F. SIDOROFF, *Formulation et identification de lois de comportement pout toles minces en emboutissage*, Rapport Ecole Centrale de Lyon, 1988.
2. M. ROUSSET, *Surface seuil de plasticité. Détermination automatique et modélisation*, Thèse de Docteur Ingénieur, Université Paris, 6, 1985.
3. H. D. BUI, *Etude de l'évolution de la frontiére du domaine èlastique avec l'ècrouissage et relation de comportement elastoplastique des mètaux cubiques*, Thèse, Faculté des Sciences, CNRS AO 2883, Paris 1969.
4. J. P. CORDEBOIS and M. BOUCHER, *Evolution des surfaces seuil en chargements complexes: aspects theorique et expèrimental*, Rapport IRSID, RE 90309 PPM/QC.
5. Rapport GIS "Mise en forme", MEF/33, IRSID-SG, 1989.
6. H. LE GAC, *Evolution de la contrainte d'écoulement et de l'anisotropic d'une tôle mince lors d'une sollicitation en expension*, Rapport IRSID, PE 3876 HLG/OS.
7. R. H. WAGONER and J. V. LAUKONIS, Metall. Trans., **14A**, 1497, 1983.

LABORATOIRE DE MECANIQUE ET TECHNOLOGIE, ENS, CACHAN
and
CNAM, PARIS, FRANCE.

Received September 3, 1991.